

## Influence of noise on periodic attractors in the Lorenz model: Zero-frequency spectral peaks and chaos

I. I. Fedchenia\*

*School of Physics and Materials, Lancaster University, Lancaster, LA1 4YB, United Kingdom*

R. Mannella

*Dipartimento di Fisica, Universita di Pisa, Piazza Torricelli 2, 56100 Pisa, Italy*

P. V. E. McClintock, N. D. Stein, and N. G. Stocks

*School of Physics and Materials, Lancaster University, Lancaster LA1 4YB, United Kingdom*

(Received 9 March 1992)

The influence of weak external noise on the Lorenz model has been studied in parameter ranges where it is characterized by pairs of nonsymmetrical periodic attractors. The investigations, based on electronic analog and digital techniques, have shown that the noise can give rise to pronounced zero-frequency spectral peaks of complicated shape and to chaos.

PACS number(s): 05.40.+j, 05.45.+b

### I. INTRODUCTION

It has been shown both theoretically [1,2] and experimentally [3] that when dynamical systems with coexisting stationary attractors (e.g., bistable systems) are perturbed by weak external noise, zero-frequency peaks appear in the spectral densities of their fluctuations. Such peaks are Lorentzian in shape and have widths defined by the reciprocal transition probability of jumps [4] between the attractors. Zero-frequency peaks have also been observed [5] for periodically driven bistable systems in the chaotic regime. It appears likely that this phenomenon is universal in character, so that it might be expected to manifest itself in *any* situation where noise induces transitions between coexisting states.

In the more complicated attractors of higher-dimensional systems, however, we will see that a quite different mechanism can also contribute to the formation of zero-frequency peaks. Even if the motions within each individual attractor of a coexisting pair (or set) of periodic attractors are of the same frequency, the dephasing effect of jumps between them will interrupt the periodicity of the wave form. In such a situation we might expect to observe a phenomenon rather similar in form to that of the chaos induced by the external perturbation of homoclinic orbits [6] when the applied fluctuations result in a random sequence of pulses, each of which corresponds to motion along one half of the homoclinic orbit. It was shown recently that for white ( $\delta$ -correlated) noise, the latter type of phenomenon can be detected through studies of power spectra [7] and Lyapunov exponents [8]. Erratic motion of a very similar kind has also been observed [9] in a one-dimensional system perturbed by simultaneous periodic and random fluctuations, even though the unperturbed system possessed no homoclinic structure.

In the present paper we extend these investigations to the Lorenz system [10]. We present and discuss the results of analog electronic and digital computer simulations of noise-induced jumps between pairs of its nonsym-

metric stable orbits. In the course of this work we have observed zero-frequency peaks of non-Lorentzian shape in the power spectra of the system, and we have found evidence that the random motion giving rise to these peaks differs substantially from stochastic motion of the Brownian type; it is, however, strikingly similar to the erratic motion generic to systems with deterministic chaotic behavior.

### II. NONSYMMETRIC ORBITS IN THE LORENZ MODEL

It is well known [10] that the Lorenz system

$$\dot{x} = -\sigma(x-y), \quad \dot{y} = rx - y - xz, \quad \dot{z} = -bz + xy, \quad (1)$$

with the standard values  $\sigma = \frac{8}{3}$  and  $b = 10$ , exhibits chaotic dynamics over a very large range of the control parameter  $r$ . This behavior is well illustrated by the results of Fig. 1, where the largest Lyapunov exponent  $\lambda_1$ , obtained from  $z(t)$  in a digital simulation, is plotted as a function of  $r$ . A positive value of  $\lambda_1$  is considered to be the signature of chaotic dynamics. There are a number of places, however, where  $\lambda_1$  dips down to zero. These are the well-known [10] periodic windows in which the motion is nonchaotic. (It should be noted that a plot such as Fig. 1 cannot be expected to reveal *all* such periodic windows because of their extreme narrowness, combined with the necessarily finite step size in  $r$ : details of the digital simulations and their analysis are given below. The number of windows is in reality infinite [10].)

The periodic orbits within the nonchaotic windows are of two distinct kinds: the symmetric type of orbit, which, when it exists, is the only attractor of the system, and nonsymmetric orbits, which always exist in pairs. In the latter case, the system is bistable. We have studied jumps between these nonsymmetric orbits induced by a single white-noise source of intensity  $D$  in the first equation

$$\dot{x} = -\sigma(x-y) + \eta(t), \quad \langle \eta(t)\eta(t') \rangle = 2D\delta(t-t'). \quad (2)$$

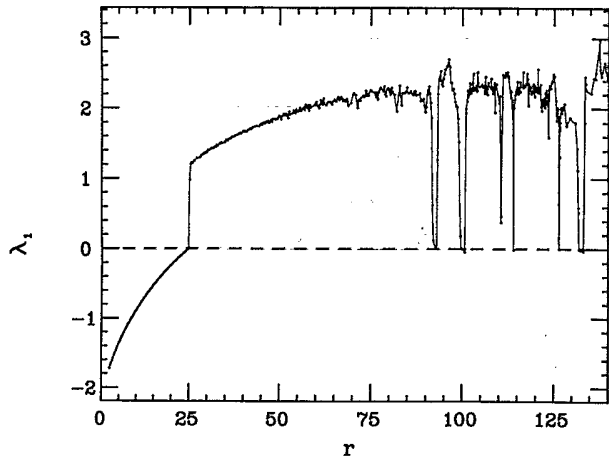


FIG. 1. Largest Lyapunov exponent  $\lambda_1$ , for the Lorenz system (1) with  $\sigma = 10$  and  $b = \frac{8}{3}$ , determined (points) by means of a digital simulation as a function of the control parameter  $r$ ; the line connecting the points is a guide to the eye. A positive value of  $\lambda_1$  implies that the motion is chaotic.

The effects of using a greater number of noise sources, or of inserting the single noise source in one of the other equations, were also investigated and found to yield results that were qualitatively the same. The two particular pairs of orbits under investigation are illustrated in Fig. 2 in the form of (computed)  $xy$  projections for zero noise intensity: those for  $r = 100$  are shown in (a) and (b), and the ones for  $r = 126.49$  are shown in (c) and (d).

The analog electronic circuit, built to standard design principles [11], could be adjusted to set  $r$  as nominally

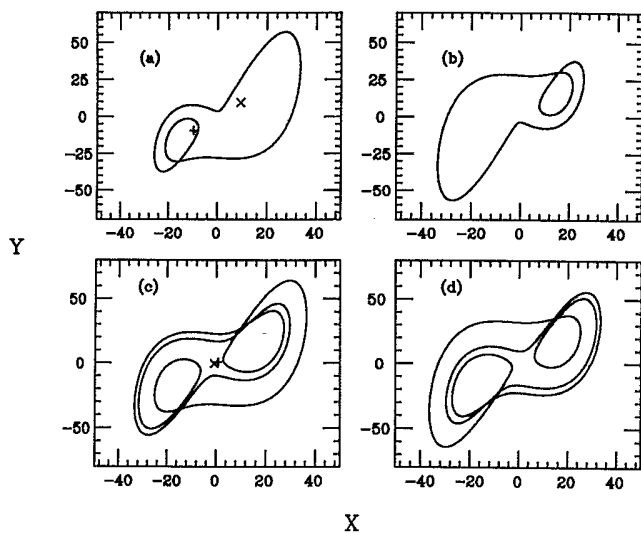


FIG. 2. Plots (a) and (b) show the computed  $x$ - $y$  projections of the pair of Lorenz periodic attractors for  $r = 100.00$ . The cross and plus symbols in (a) indicate the positions of the centers of mass for (a) and (b), respectively, which differ significantly from each other. Plots (c) and (d) provide the corresponding information for the pair of attractors at  $r = 126.49$ ; note that their centers of mass are almost coincident.

equal to one of the required values, and then fine-tuned until the displayed  $xy$  phase projection corresponded to the required orbit. Some typical  $x(t)$  signals from the circuit after filtration of high frequencies are shown in Figs. 3 and 4; a low-pass filter was used to emphasize jumps and phase discontinuities at the fundamental frequency, and correspondingly to deemphasize the effect of harmonics arising from the multiple loops within one cycle of the orbit.

The periodic part of the motion in Figs. 3 and 4 represents motion within one of the attractors. The intermittent jumps in Fig. 3 represent noise-induced transitions between attractors. The time constant of the relaxation is that of the low-pass filter, but the amplitude of the relaxation relates to the difference in the  $x$  projection of the centers of mass for the attractors of a pair. This difference is significant for the attractors at  $r = 100$ , but close to zero for those at  $r = 126.49$ , which is why the large relaxation effects are seen in the former case but not

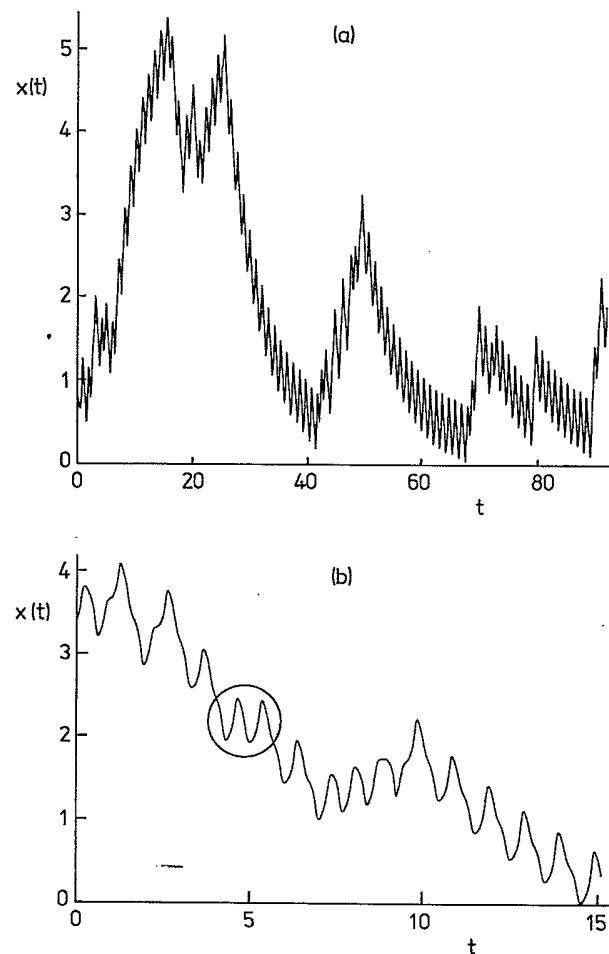


FIG. 3. Typical  $x(t)$  time series (arbitrary ordinate scale) from the electronic model, after filtration of high frequencies for  $r = 100$ . The abscissa scale is in terms of the dimensionless time units of Eq. (1). The plot in (b) represents an expanded view as compared to that in (a). Jumps between orbits manifest themselves as changes in the direction of relaxation. Jumps of phase within an individual orbit take place without change of relaxation direction, as shown by the circled example in (b).

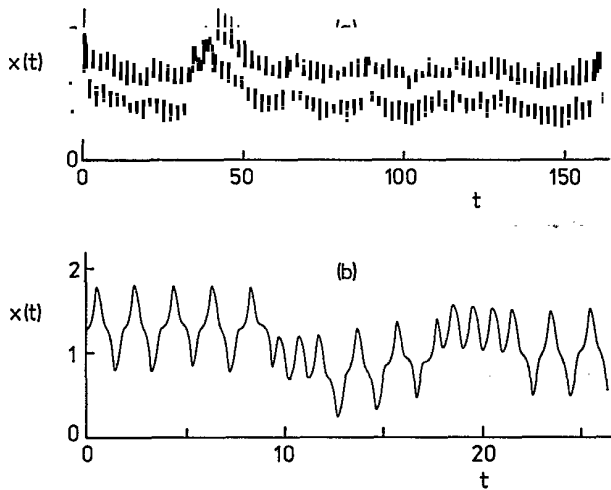


FIG. 4. Typical  $x(t)$  time series (arbitrary ordinate scale) from the electronic model, after filtration of high frequencies for  $r=126.49$ . The abscissa scale is in terms of the dimensionless time units of Eq. (1). The plot in (b) represents an expanded view, as compared to that in (a).

(see Fig. 4) in the latter. Jumps to the orbit of opposite symmetry are also manifested by discontinuities in the phase of the periodic motion; it is also evident from the data [e.g., circled part of Fig. 3(b)] that phase jumps can occur during an orbit *within* one attractor.

The general expression for the zero-frequency peak in the power spectral density of such signals, obtained in the Appendix, is

$$S(\omega) = \frac{n\omega^2}{\Lambda^2 + \omega^2} \frac{\Delta^2}{\lambda^2 + \omega^2} + m|\Pi|^2, \quad (3)$$

where  $n$  and  $m$  are respectively the average number of jumps between orbits and the average number within orbits, per unit time;  $\Lambda^{-1}$  is the average time between interorbit jumps;  $\Delta$  is the distance between the centers of mass;  $\lambda$  is the relaxation constant; and  $|\Pi|^2$  is the spectrum of the periodic component in a half period.

It is evident from (3) that the dependence of  $S(\omega)$  on external noise intensity is complicated by mutually competitive processes. It is intuitively reasonable, however,

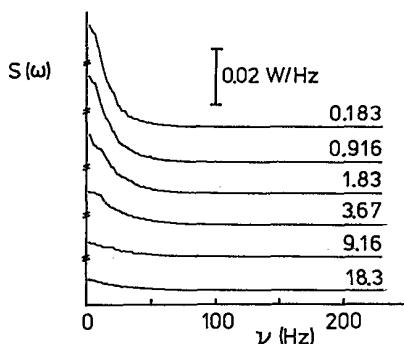


FIG. 5. Zero-frequency power spectral peaks measured for the electronic model with  $r=100$  for various intensities  $D$  of external noise, as indicated.

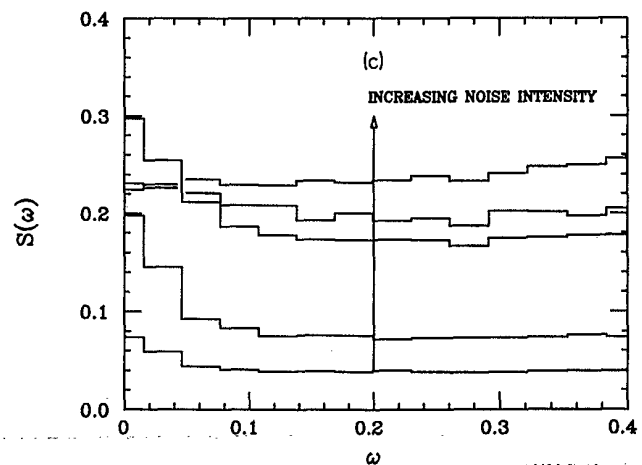
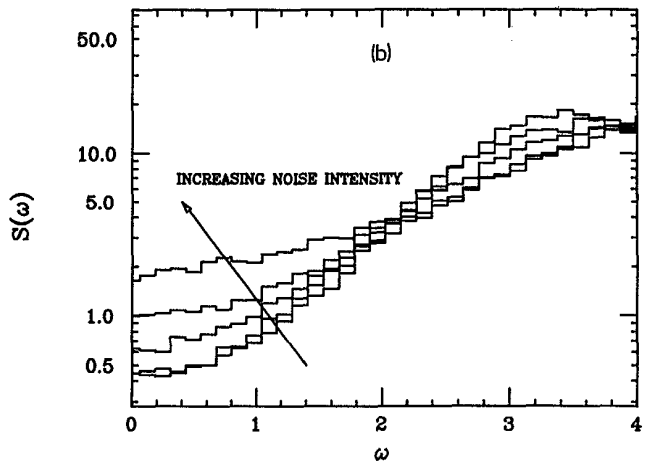
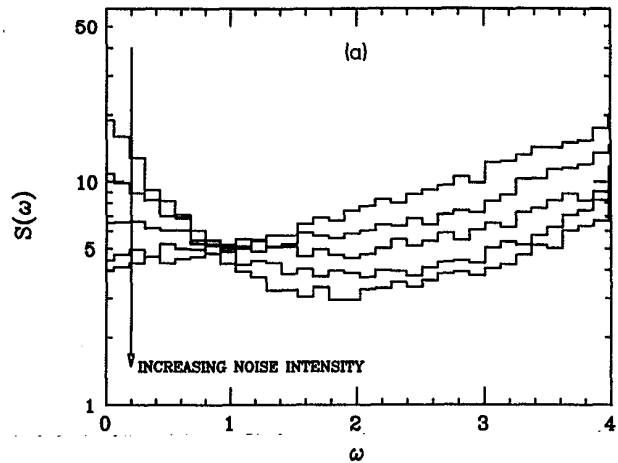


FIG. 6. Low-frequency power spectra determined from the digital simulation for various intensities of external noise ( $D=0.1, 0.3, 1.0, 3.0, 10.0$ ): (a)  $r=100$ ; (b)  $r=126.49$ . The plot in (c) shows the result of a separate digital simulation for  $r=126.49$ , seeking evidence for a zero-frequency peak, which is clearly evident in the results. The noise intensities used, denoted at the position of the arrow, were  $D=1.0 \times 10^{-5}; 3.0 \times 10^{-5}; 6.0 \times 10^{-5}; 1.0 \times 10^{-4}; 1.0 \times 10^{-3}$ .

to guess that for the orbit with  $r=100$  [Figs. 2(a), 2(b), and 3] the zero-frequency peak will broaden and diminish with increasing noise intensity due to the relatively large  $\Delta$  and the rapid increase of  $\Lambda$ . For the orbit with  $r=126.49$ , on the other hand [Figs. 2(c), 2(d), and 4],  $\Delta \approx 0$  and the second mechanism involving the term

$$S(\omega) \approx m |\Pi|^2 \quad (4)$$

due to periodicity violation may be expected to dominate. The power spectrum in this latter case should, if anything, increase with increasing noise intensity due to the rapid growth of  $m$ , corresponding to the rate of jumping between two points on the same orbit, because every such jump implies a break in the periodic sequence: see Fig. 3.

Some examples of low-frequency power spectra measured for the analog electronic model for a series of noise intensities are shown in Fig. 5. The results for  $r=100$  show very much the type of behavior expected: there is a pronounced zero-frequency peak that broadens with increasing noise intensity owing to the increased rate of hopping between the attractors. For  $r=126.49$ , on the other hand, the peak was weaker by a factor of  $\sim 10^3$  and its variation with noise intensity was in the opposite direction. The extremely small power in the peak strongly suggested that it might, in fact, merely represent an artifact of the low-pass filtering. This idea was confirmed by performing digital simulations of the same system, using the raw (unfiltered) signal.

The digital simulations were carried out using the algorithm of Ref. [12]. The integration time step was kept very small and was typically  $\sim 10^{-3}$  of the period of revolution around the attractor. Examples of the low-frequency power spectra obtained in this way are shown in Fig. 6. It is immediately evident from Fig. 6(a) that the existence of a zero-frequency peak for  $r=100$  is confirmed; but Fig. 6(b) apparently shows that there is no such peak for  $r=126.49$ . It appears, therefore, that the effect of the phase discontinuities resulting from interorbit and intraorbit hopping in the latter case is just not large enough to produce a maximum at  $\omega=0$  for the unfiltered signal, at least within the resolution provided by the simulations. This inference was tested by performing a new digital simulation with enhanced statistics, concentrating especially on the shape of the spectral density at low frequencies. The result is shown in Fig. 6(c). It is evident that there is indeed a very weak zero-frequency peak that at first increases with increasing  $D$ , but is quickly overcome by the low-frequency tail of the maximum due to the periodic part of the motion.

It is found that the shape of the zero-frequency peaks for  $r=100$  [Figs. 5 and 6(a)] is neither Lorentzian as in [1, 2], nor exponential as in [6, 7]; it appears, rather, to be a combination of such line shapes just as (3) would imply.

### III. CHAOTIC AND STOCHASTIC MOTION

The periodic perturbation of a homoclinic orbit can induce chaotic behavior in a system [6, 8]. A rather similar response in terms of the low-frequency power spectra can also be induced by external white noise [7, 8]. It was suggested in [13] that chaotic and stochastic motion could be

distinguished from each other by analysis of the high-frequency wings of their spectral peaks, a Lorentzian shape being generic for stochastic motion and an exponential one for chaotic motion. From this point of view, (3) suggests that the spectra of noise-induced jumps between two antisymmetric orbits should be regarded as being composed of a mixture of stochastic and chaotic components. It is therefore of some interest to investigate the nature of the chaos that is induced in the system.

The character of the dynamics was investigated by determination of its Lyapunov exponents [14] for the case of the digital simulation. Figure 7 shows the variation of the largest Lyapunov exponent  $\lambda_1$  with  $r$  for several different noise intensities within and close to the periodic window near  $r=126.49$ . (We indicate the three Lyapunov exponents of the system, in decreasing order, by  $\lambda_1$ ,  $\lambda_2$ , and  $\lambda_3$ , respectively.) It is immediately evident that even the weakest noise intensity causes the width of the window to shrink, and as the noise intensity increases further, it disappears altogether and  $\lambda_1$  then becomes positive throughout the region plotted. For the strongest noise intensity, nothing remains of the periodic window except a slight dip in  $\lambda_1$  at the relevant values of  $r$ . This suggests that the dynamics induced by the noise is indeed chaotic and that we are dealing with another example of "noise-induced chaos" rather similar to that discussed in [8], albeit for a totally different kind of system. The origin of this interesting phenomenon is not yet fully understood. A possible explanation is that the noise can transiently drive the system away from its stable periodic orbit towards neighboring (unstable) chaotic orbits, which it then follows briefly before returning again. Consistent with this idea, the change from nonchaotic to chaotic behavior occurs in a relatively gradual way as the noise intensity is increased, which would cause such excursions to become correspondingly more frequent. Figure 8 plots the variation of the three Lyapunov exponents as a function of noise intensity for  $r=126.5$  in the middle of the periodic window. It can be seen that for noise intensity

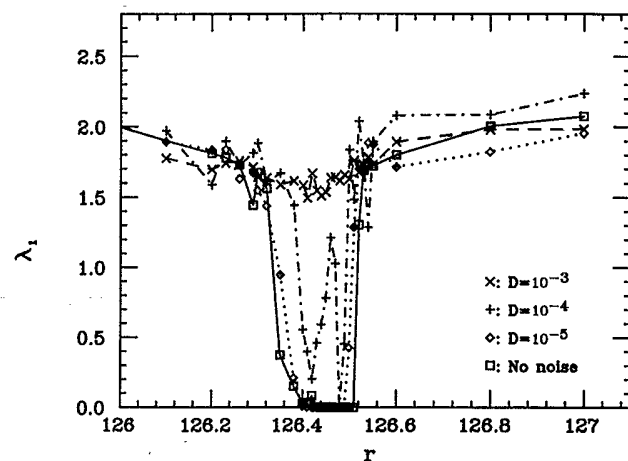


FIG. 7. Effect of external noise on the largest Lyapunov exponent  $\lambda_1$ , in the vicinity of the periodic window at  $r=126.49$ :  $\lambda_1$  is plotted as a function of  $r$  for the indicated noise intensities; the lines are guides to the eye.

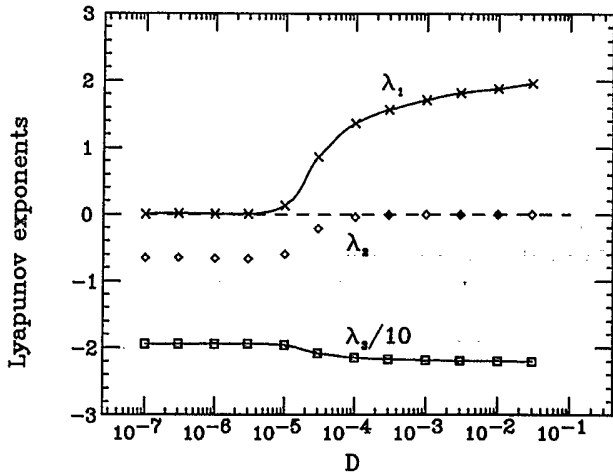


FIG. 8. Three Lyapunov exponents  $\lambda_1, \lambda_2, \lambda_3$  plotted as function of noise intensity for  $r=126.5$  near the middle of a periodic window. Note that  $\lambda_3$  has been scaled down by a factor of 10.

above  $\sim 10^{-5}$ ,  $\lambda_1$  gradually rises toward the value of 2 seen outside the periodic window (see Fig. 1). The exponent corresponding to perturbations parallel to the attractor is always zero. Even in the presence of noise, the stretching of such perturbations will be diffusive (proportional to  $\sqrt{t}$ ) rather than depending exponentially on  $t$ . This role is initially played by  $\lambda_1$ , subsequently by  $\lambda_2$ . The three exponents should sum to  $-(\sigma + b + 1)$ , the divergence of the flow in phase space, at least in the limit of zero noise. Since this equality is only reasonably well satisfied by the measured exponents, the small negative change that appears to occur in  $\lambda_3$  is unlikely to be significant.

#### IV. CONCLUSION

We have studied the influence of weak external noise on the Lorenz model in parameter ranges where it is characterized by pairs of nonsymmetric attractors. The noise results in jumps between and within the attractors, possessing both chaotic and stochastic features. The corresponding spectral densities for  $r=100$  exhibit narrow zero-frequency peaks of complicated shape that are consistent with (3); those for  $r=126.49$  exhibit only negligible peaks at zero frequency, as shown in Fig. 6(c). The distinction is readily understandable in terms of the difference in the center of motion (Fig. 2) between each pair of attractors, which is significant for  $r=100$  and near zero for  $r=126.49$ . The variation of the largest Lyapunov exponent with noise intensity (Figs. 7,8) provides a convincing demonstration that the system exhibits noise-induced chaos. Although the latter phenomenon obviously differs from its deterministic equivalent in that the chaos disappears as the noise intensity tends to zero, it must of course also be borne in mind that all real systems are inevitably subject to noise, both of environmental origin and arising from internal fluctuations (e.g., thermal noise, or from spontaneous emission in the case of a laser).

We are grateful to Professor M. Giordano for access to his computing facilities and to Professor H.D.I. Abarbanel for making available his code for the computation of Lyapunov exponents. The work was supported by the Istituto Nazionale Fisica della Materia (Italy) and by the Science and Engineering Research Council (United Kingdom).

#### APPENDIX

To calculate the power spectrum of the signals depicted in Figs. 3 and 4 we use the construction proposed in Ref. [6] but point out first that the signal is equivalent to the pulse sequence

$$x(t) = \sum_{n=1}^{\infty} (-1)^n s(t-t_n) + \sum_{j=1}^{\infty} (-1)^j p(t-t_j), \quad (\text{A1})$$

$$s(t) = \Delta e^{-\lambda t} \Theta(t),$$

where  $\Delta$  is the distance between the two steady states;  $\lambda$  is the relaxation constant towards these steady states;  $\Theta(t)=1$  for  $t>0$  and  $\Theta(t)=0$  for  $t<0$ ;  $p(t-t_j)$  is the periodic orbit with period  $\tau$ ;  $t_n$  is the random sequence of times corresponding to jumps between the two orbits; and  $t_j$  is the random sequence of times corresponding to all jumps of phase of the periodic component due both to jumps between the attractors and also to jumps of phase inside one and the same orbit. The random variable  $a_j$  takes values 0 and 1. Introducing the window function

$$\xi_T(t) = \begin{cases} 1, & 0 \leq t \leq T \\ 0, & t > T, t < 0 \end{cases} \quad (\text{A2})$$

and rewriting the expression for the signal in terms of the convolution integral

$$x_T(t) = \int_{-\infty}^{\infty} dt' [\alpha_T(t-t')s(t') + \beta_T(t-t')p(t')], \quad (\text{A3})$$

where

$$\alpha_T(t) = \xi_T(t) \sum_{n=1}^{\infty} (-1)^n \delta(t-t_n), \quad (\text{A4})$$

$$\beta_T(t) = \xi_T(t) \sum_{j=1}^{\infty} (-1)^j \delta(t-t_j),$$

we readily obtain the power spectrum

$$S(\omega) = \lim_{T \rightarrow \infty} \frac{1}{T} \langle |\hat{\alpha}_T(\omega)|^2 |\hat{\beta}_T(\omega)|^2 + |\hat{\beta}_T(\omega)|^2 |\Pi(\omega)|^2 \rangle. \quad (\text{A5})$$

We have assumed that phase jumps are statistically independent of jumps between the two orbits. Carets denote Fourier transforms and  $\Pi(\omega) = \int_{-\tau/2}^{\tau/2} e^{i\omega t} p(t) dt$  is the Fourier transform of one-half period of the periodic component. If  $N$  interorbit jumps and  $M$  phase jumps occur in time  $T$ , we have

$$\hat{\alpha}_T(\omega) = \sum_{n=1}^{N/2} \exp(-i\omega t_{2n}) - \exp(-i\omega t_{2n-1}), \quad (\text{A6})$$

$$\hat{\beta}_T(\omega) = \sum_{j=1}^M (-1)^j \exp(-i\omega t_j).$$

The assumption that the time between two interorbit jumps  $\Delta t$  has an exponential distribution  $p(\Delta t) = \Lambda \exp(-\Lambda \Delta t)$ , and that phase jumps are uniformly distributed, allows the averages to be performed

$$\lim_{T \rightarrow \infty} \left\langle \frac{1}{T} |\hat{\alpha}_T(\omega)|^2 \right\rangle = \frac{n\omega^2}{\Lambda^2 + \omega^2}, \quad (\text{A7})$$

$$\lim_{T \rightarrow \infty} \left\langle \frac{1}{T} |\hat{\beta}_T(\omega)|^2 \right\rangle = m,$$

where  $n$  is the average number of jumps between the two orbits per unit time, and  $m$  is the average number of phase jumps per unit time. Use of the result

$$|\hat{s}(\omega)|^2 = \frac{\Delta^2}{\lambda^2 + \omega^2}$$

gives the final expression

$$S(\omega) = \frac{n\omega^2}{\Lambda^2 + \omega^2} \frac{\Delta^2}{\lambda^2 + \omega^2} + m |\Pi|^2. \quad (\text{A8})$$

When  $\Lambda = 0$  and there are no phase jumps, (A8) takes the form of the zero-frequency peak from [1–3]: the only difference is the prefactor  $n$ , the number density of jumps [15], which is a quantity easily measured in experiment. Where jumps between the two attractors can be regarded as instantaneous and the distance  $\Delta$  between them equal to zero, we recover the results of [6].

\*Permanent address: Institute of Physics, Byelorussian Academy of Sciences, Minsk, CIS. Now at Department of Physical Chemistry, Umea University, Umea 90187, Sweden.

- [1] M. I. Dykman, S. M. Soskin, and M. A. Krivoglaz, *Physica* **133A**, 53 (1985).
- [2] K. Voigtlaender and H. Risken, *J. Stat. Phys.* **40**, 397 (1985); H. Risken and K. Voigtlaender, *ibid.* **41**, 825 (1985).
- [3] M. I. Dykman, R. Mannella, P. V. E. McClintock, F. Moss, and S. M. Soskin, *Phys. Rev. A* **37**, 1303 (1988).
- [4] P. Hanggi, P. Talkner, and M. Borkovec, *Rev. Mod. Phys.* **62**, 251 (1990).
- [5] F. T. Arecchi and F. Lisi, *Phys. Rev. Lett.* **49**, 94 (1982).
- [6] V. Brunson and P. Holmes, *Phys. Rev. Lett.* **58**, 1699 (1987).
- [7] E. F. Stone, *Phys. Lett. A* **148**, 434 (1990).
- [8] A. R. Bulsara, E. W. Jacobs, and W. C. Schieve, *Phys. Rev. A* **42**, 4614 (1990).
- [9] Z.-Y. Chen, *Phys. Rev. A* **42**, 5837 (1990).
- [10] C. Sparrow, *The Lorenz Equations: Bifurcations, Chaos and Strange Attractors* (Springer-Verlag, Berlin, 1982).
- [11] L. Fronzoni in *Noise in Nonlinear Dynamical Systems*, edited by F. Moss and P. V. E. McClintock (Cambridge University Press, Cambridge, 1989), Vol. 3, p. 222; P. V. E. McClintock and F. Moss, *ibid.* p. 243.
- [12] R. Mannella in *Noise in Nonlinear Dynamical Systems* (Ref. [11]), p. 189; R. Mannella and V. Palleschi, *Phys. Rev. A* **40**, 3381 (1989).
- [13] D. Sigeiti and W. Horsthemke, *Phys. Rev. A* **35**, 2276 (1987).
- [14] A. Wolf, J. B. Swift, H. L. Swinney, and J. A. Vastano, *Physica D* **16**, 285 (1985). For a refined technique for the extraction of Lyapunov exponents from a time series, see P. Bryant, R. Brown, and H. D. I. Abarbanel, *Phys. Rev. Lett.* **65**, 1523 (1990) and R. Brown, P. Bryant, and H. D. I. Abarbanel, *Phys. Rev. A* **43**, 2787 (1991).
- [15] R. L. Stratonovich, *Topics in the Theory of Random Noise* (Gordon and Breach, New York, 1963).